

# Impact of Landuse Change on Surface Temperature in Ibadan, Nigeria

Abegunde Linda, Adedeji Oluwatola

**Abstract**—It has become an increasing evident that large development influences the climate. There are concerns that rising temperature over developed areas could have negative impact and increase living discomfort within city boundaries. Temperature trends in Ibadan city have received little attention, yet the area has experienced heavy urban expansion between 1972 and 2014. This research aims at examining the impact of landuse change on surface temperature knowing that the built-up environment absorb and store solar energy, resulting into the Urban Heat Island (UHI) effect. The Landsat imagery was used to examine the landuse change for a period of 42 years (1972-2014). Land Surface Temperature (LST) was obtained by converting the thermal band to a surface temperature map and zonal statistic analyses was used to examine the relationship between landuse and temperature emission. The results showed that the settlement area increased to a large extent while the area covered by vegetation reduced during the study period. The spatial and temporal trends of surface temperature are related to the gradual change in urban landuse/landcover and the settlement area has the highest emission. This research provides useful insight into the temporal behavior of the Ibadan city.

**Keywords**—Landuse, LST, Remote sensing, UHI.

## I. INTRODUCTION

GLOBAL warming increase is believed to be as a result of landuse/landcover change [3]. Urbanization and urban sprawl are the dominant factors in regional landscape evolution across the world, which affects climate leading to great environmental impact. Rapid urbanization results from the large-scale development of commercial, manufacturing and transportation areas, which leads to the emergence of the Urban Heat Island (UHI) effect. Urban Heat Island is a typical phenomenon of urban climates that challenge sustainable livelihood and describes the excess temperature near the ground (canopy layer) of the central urban locations as being higher than those of nearby or surrounding areas of similar elevation [11]. The characteristics of the UHI are related to both the intrinsic nature of the city, such as its size, population, building density and land uses, and external factors such as climate and weather [9]. The process of urbanization produces radical changes in the nature of the surface and atmospheric properties of a region. It involves the transformation of radiation, thermal, moisture and aerodynamic characteristics, and thereby dislocates the natural solar and hydrologic cascades. UHI has been regarded as a

well-documented example of anthropogenic climate modifications within the field of urban climate [1].

One of the possible causes of UHI is the drastic reduction in the greenery areas of the cities, and increase in built-up areas brought about by population increase which can be observed in Ibadan, a rapidly developing city in Nigeria. Urban areas in Nigeria will generally experience the same exposures to climate as their surrounding country side, the urban setting- its form and socio-economic activity can alter exposure as well as impact at the local scale. Built-up areas in the cities create unique micro-climate due to the replacement of natural vegetation with artificial surfaces. This affects air temperature, wind direction and precipitation patterns, amongst others. The impact of heat waves is particularly strong in cities and towns which lead to decrease in water resource quality and quantity, increase risk of forest fire, decrease cold-related human morbidity and mortality along with reduced heating energy demand, increase flood, landslide, avalanche, and mudslide damage. There are also expected to be some indirect effects due to crop damage by heat, water or pests and increased migration pressure as people move to more climatologically acceptable regions [6]. If the relationship between city form and the extent of the UHI were known, it would be possible to identify thermally efficient models of urban development. The availability of remotely sensed data makes the research more achievable. A satellite-based methodology is used to estimate urban temperatures and to classify various landuses. Remotely-sensed thermal imagery can provide a time-synchronized grid of temperature data over a whole city, and distinctive differences in the temperatures of individual buildings [8]. The objective of this research is to integrate satellite data in analyzing urban heat island effects in Ibadan city. Landuse and temperature distributions derived from satellite data, and a Geographical Information System (GIS) are used to visualize and analyze the interactions between temperature and landuse based on the following objectives: analyzing the changes in landuse/landcover pattern; analyzing the urban heat intensity using Landsat imagery; and examining the relationship between UHI and landuse.

## II. STUDY AREA

Ibadan city is located between latitudes  $7^{\circ}20'$  and  $7^{\circ}26'$  of the equator and longitudes  $3^{\circ}48'$  and  $3^{\circ}56'$  of the Greenwich meridian. It is directly connected to many towns as its rural hinterland by a system of roads, railways and air routes. The city is the dominant urban centre in Oyo State, the largest indigenous city in West Africa and has an overall population density of 586 persons per  $\text{km}^2$ . The administrative and

L.O. Abegunde is with the National Centre for Remote Sensing, Plateau State, Nigeria (phone: +2348101204335; e-mail: lindaabegunde@yahoo.com).

O. Adedeji is with the Institute of Ecology and Environmental Study, Obafemi Awolowo University, Osun State, Nigeria (e-mail: oluwatola2002@yahoo.com).

commercial importance of Ibadan has resulted in the land being a key investment asset. Ibadan enjoys the characteristics of West African Monsoonal climate, marked by distinct seasonal shift in wind pattern just because of its latitudinal location. Between the rainy season periods of March to October, the city is under the influence of the moist maritime south-west monsoon winds which is below the inland from the Atlantic Ocean. The dry season occurs from November to February when the dry dust-laden winds blow from the Sahara desert.

Ibadan has grown so rapidly that within a period of only 150 years, it has become one of the greatest metropolitan areas in Africa. Since the country became independent, Ibadan had utilized not only the initial advantage acquired as headquarter of the old western region but also harnessed its location advantage to continue the domination of commerce in the old western Nigeria. Thus, in spite of the decentralization of civil service employment following the creation of states in 1976 and 1991, Ibadan remains a major commercial, educational and administrative centre in Nigeria, and recent years has embarked upon improving its industrial base.

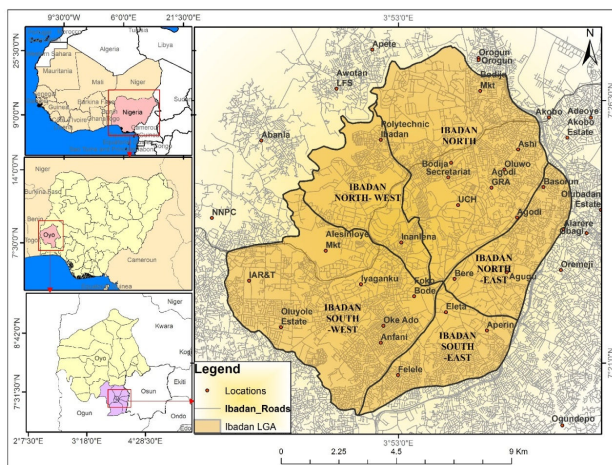


Fig. 1 Study Area Map

### III. METHODOLOGY

The Landsat data were acquired from the global landcover website at the University of Maryland, USA [12]. They are Multispectral Scanner (MSS) image for 15<sup>th</sup> Dec., 1972, Thematic Mapper (TM) image for 18<sup>th</sup> Dec., 1984, Enhance Thematic Mapper plus (ETM+) image for 6<sup>th</sup> Feb., 2000 and 6<sup>th</sup> Dec., 2006, and the Operational Land Imager (OLI) for 5<sup>th</sup> Feb., 2013. The satellite data have 30m spatial resolutions, and the TM and ETM+ images have spectral range of 0.45-2.35 micrometer with bands 1 to 8 while the Operational Land Imager (OLI) extends to band 12.

A False Colour Composite (FCC) operation were performed using the Idrisi software and the Landsat were combined in the order of band 4, band 3 and band 2 for Landsat TM and ETM+ while that of Landsat OLI was in the order of band 5, band 4 and band 3 due to change in sensor. The FCC was further classified using the Maximum Likelihood classification

technique. A supervised classification was performed by creating a training sample, and based on spectral signature curve, various landuse classes were created namely: low and high density settlement area, waterbody, forest and vegetation.

The thermal band (10.4-12.5  $\mu\text{m}$ ) of the Landsat ETM+ sensor was used to derive LSTs over the study area [7]. For the Landsat ETM+ sensor, images in the thermal band are captured twice: one in the low-gain mode (band 6L) and the other in the high-gain mode (band 6H). Band 6L is used to image surfaces with high brightness, whereas band 6H is for low brightness [5]. Band 6H was used in this study. The DN's of band 6H from the Landsat ETM, ETM+ image and band 11 for Landsat OLI were first converted to spectral radiance using:

$$L = LMIN + (LMAX - LMIN) * DN \div 255 \quad (1)$$

where: L is the spectral radiance at the sensor's aperture in  $\text{Wm}^{-2}\text{sr}^{-1}\mu\text{m}^{-1}$ ; LMIN is the spectral radiance that is scaled to QCALMIN (3.2  $\text{Wm}^{-2}\text{sr}^{-1}\mu\text{m}^{-1}$ ); LMAX is the spectral radiance that is scaled to QCALMAX (12.65  $\text{Wm}^{-2}\text{sr}^{-1}\mu\text{m}^{-1}$ ); QCAL is the DN; QCALMIN is the minimum quantized calibrated pixel value (corresponding to LMIN) in DN (0); and QCALMAX is the maximum quantized calibrated pixel value (corresponding to LMAX) in DN (255). Spectral radiance values for band 6H were then converted to radiant surface temperature under an assumption of uniform emissivity using pre-launch calibration constants for the Landsat ETM+ sensor implemented into [4]:

$$Tk = \frac{K2}{\ln\left(\frac{K1}{L} + 1\right)} \quad (2)$$

where Tk is radiant surface temperature (in Kelvin); K2 is calibration constant 2 (1282.71 K); K1 is calibration constant 1 (666.09  $\text{Wm}^{-2}\text{sr}^{-1}\mu\text{m}^{-1}$ ); and L is the spectral radiance at sensor in  $\text{Wm}^{-2}\text{sr}^{-1}\mu\text{m}^{-1}$ .

The calculated radiant surface temperatures were subsequently corrected for emissivity using the equation developed by [2]:

$$LST = TB \div [1 + (\lambda TB \div \rho)] \ln \epsilon \quad (3)$$

where LST is Land Surface Temperature (in Kelvin); TB is radiant surface temperature (in Kelvin);  $\lambda$  is the wavelength of emitted radiance (11.5  $\mu\text{m}$ );  $\rho$  is  $h \times c / \sigma$  (1.438  $\times 10^{-2}$  m K); h is Planck's constant (6.26  $\times 10^{-34}$  J s); c is the velocity of light (2.998  $\times 10^8$  m/sec);  $\sigma$  is Stefan Boltzmann's constant (1.38  $\times 10^{-23}$  J K<sup>-1</sup>); and  $\epsilon$  is emissivity. Finally, the LSTs were converted into Celsius (Tc) using:

$$Tc = LST - 273 \quad (4)$$

Random points were generated and the surface temperature was extracted using the ArcGIS 10.2, point located in the rural

area of Ibadan was used as reference point while the other random points were deducted from the reference point. The formula of UHI is:

$$UHI = T_u - T_r \quad (5)$$

As this paper focuses on the environmental impact of urban Landuse/landcover zoning, emissivity were corrected according to the nature of LULC. Mean surface emissivity estimates for each LULC type were derived based on the methodology presented by [10].

#### IV. RESULT

##### A. Changes in Landuse/Landcover Pattern

In 1972, high density settlement areas, located at the central area of the 5 Local Government Areas of Ibadan covers about 4.03km<sup>2</sup> of the study area which is about 0.135% and that of low density is 0.36%. Vegetation appears to be the predominant landcover type with a spatial extent of 97.07%. There appear to be pockets of bareground/rock outcrop of about 2.38% while the waterbody located north-west covers about 0.07%.

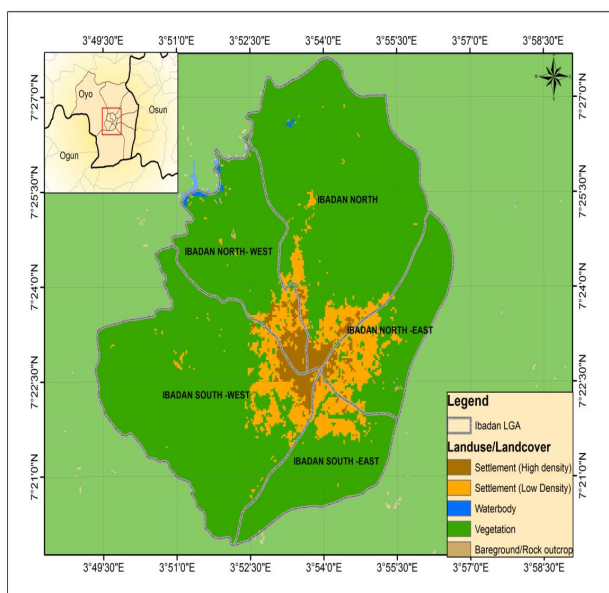


Fig. 2 LULC Classification (1972)

1984 showed increase in high density settlement area to about 9.79% due to transition from its low density areas, as growth in population has been the major cause for the increment. Low density settlement areas also increased to about 3.61% and bareground/rock outcrop to about 10.89% of the study area.

By 2000, 16 years from the previous year, settlement and bareground/rock outcrop increased further. The high density settlement areas increased to about 0.48% and the landmass covering its low density increased to about 4.9% of the study area. Vegetation decreased to about 74.3% which was 85.09%

in 1984, as the major contributing factor to the loss in vegetation appears to be as a result of settlement growth.

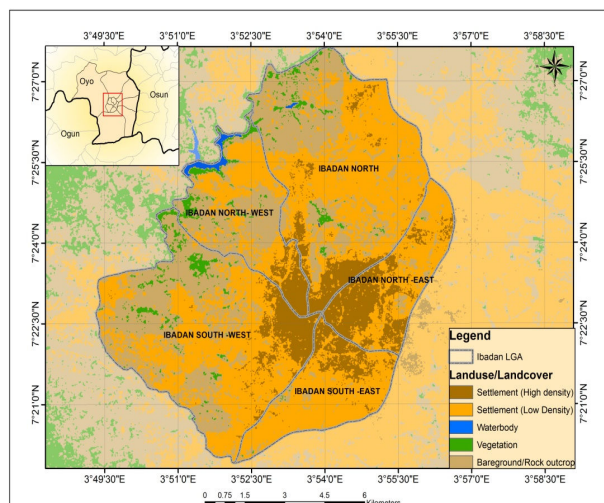


Fig. 3 LULC Classification (1984)

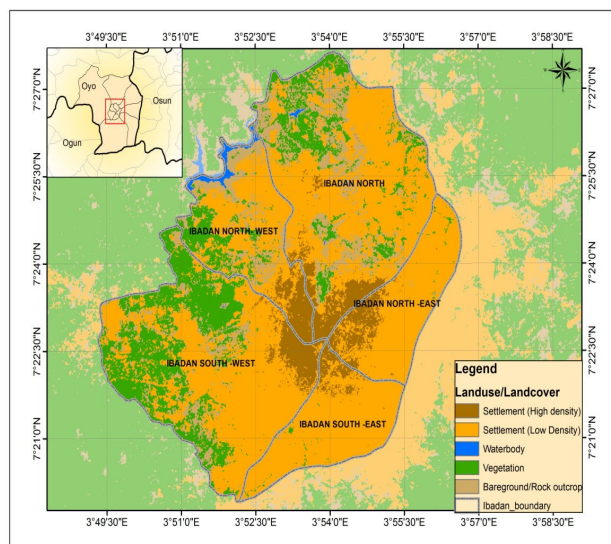


Fig. 4 LULC Classification (2000)

2006 continued to show similar trend as the previous years. There appeared to be increment in the spatial extent of bareground/rock outcrop and settlements, a steady decrease in vegetation to about 60.3% which is due to clearing of water hyacinths and other aquatic weeds as the federal government embarked on aquatic weed control project during the year.

By 2013, the low density settlement area had covered virtually all the 5 Local Government Areas to about 8.65%. The dominant vegetation type in the study area appeared to be riparian vegetation growing along the watercourse reduced to about 55.57%. Bareground/rock outcrop increased to about 35.05% and the high density settlement areas increased to about 0.69%. In general, the low and high density settlement

areas continued to increase as a result of population growth while vegetation cover reduced due to anthropogenic factors.

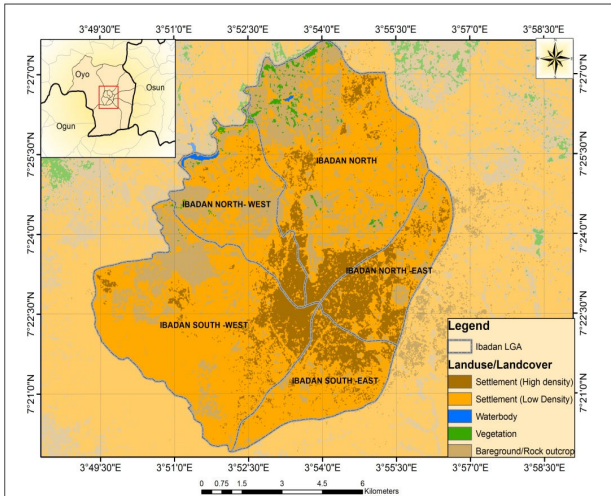


Fig. 5 LULC Classification (2006)

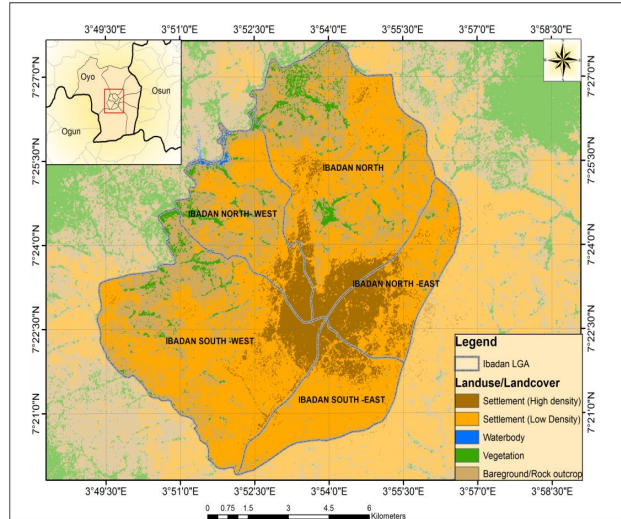


Fig. 6 LULC Classification (2013)

TABLE I  
SUMMARY OF LULC CLASSIFICATION

LULC	1972	1984	2000	2006	2013
High Density Settlement	4.03 km <sup>2</sup> (0.135%)	9.79 km <sup>2</sup> (0.31%)	15.29 km <sup>2</sup> (0.48%)	17.32 km <sup>2</sup> (0.54%)	22.27 km <sup>2</sup> (0.69%)
Low Density Settlement	11.55km <sup>2</sup> (0.36%)	115.64 km <sup>2</sup> (3.61%)	157.15 km <sup>2</sup> (4.9%)	170.48 km <sup>2</sup> (5.32%)	277.41 km <sup>2</sup> (8.65%)
Waterbody	2.34 km <sup>2</sup> (0.36%)	3.32 km <sup>2</sup> (0.1%)	0.87 km <sup>2</sup> (0.03%)	2.43 km <sup>2</sup> (0.08%)	0.83 km <sup>2</sup> (0.03%)
Vegetation	3111.42km <sup>2</sup> (97.07%)	2727.69km <sup>2</sup> (85.09%)	2381.76km <sup>2</sup> (74.3%)	1933.15km <sup>2</sup> (60.3%)	1781.45km <sup>2</sup> (55.57%)
Bareground/Rock Outcrop	76.15km <sup>2</sup> (2.38%)	349.17km <sup>2</sup> (10.89%)	650.53km <sup>2</sup> (20.29%)	1082.27km <sup>2</sup> (33.76%)	1123.69km <sup>2</sup> (35.05%)

*B. Inter-annual Variation in Surface Temperature*

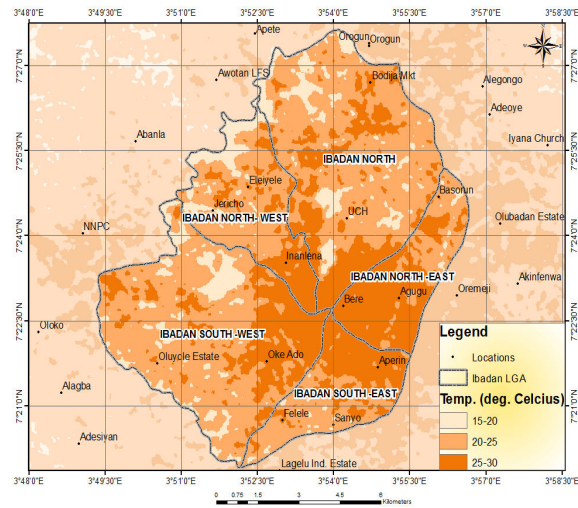


Fig. 7 Surface Temperature (1984)

In 1984, the surface temperature of the core areas are the highest which ranges between 25°-30°C while the larger portion of the area had surface temperature values ranging between 20°-25°C. Waterbody falls within the least amount of surface temperature (about 19.30°C), followed by vegetation with temperature value of about 22.20°C and settlement areas

having the highest emission of temperature values ranging over 25°C which corresponds to the principle of urban heat.

By 2000 shown in Fig. 8, more areas fell within the higher emission of surface temperature class of 25°-30°C. Areas with lower temperature correspond to waterbody and vegetation having temperature values of 20.35°C and 22.21°C respectively.

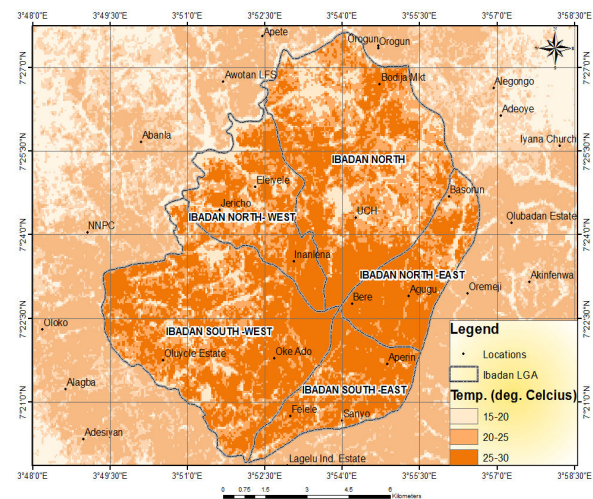


Fig. 8 Surface Temperature (2000)

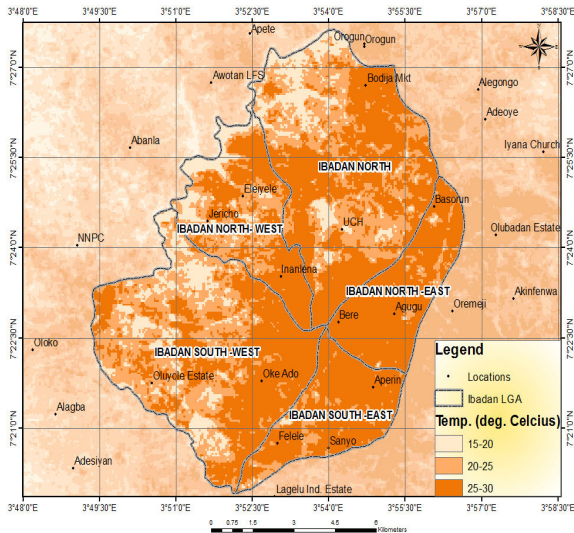


Fig. 9 Surface Temperature (2006)

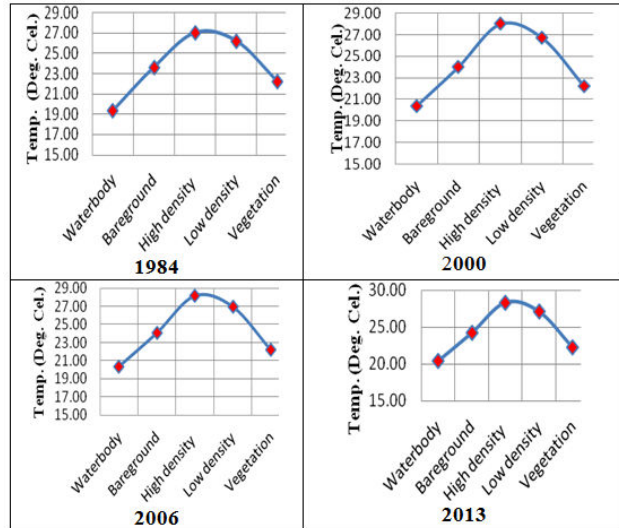


Fig. 11 Surface Temperature Values

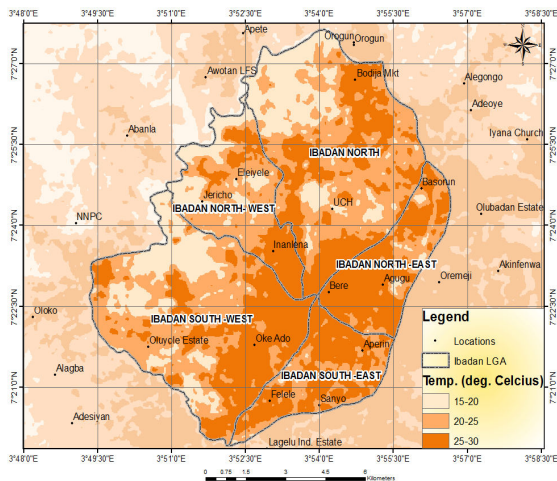


Fig. 10 Surface Temperature (2013)

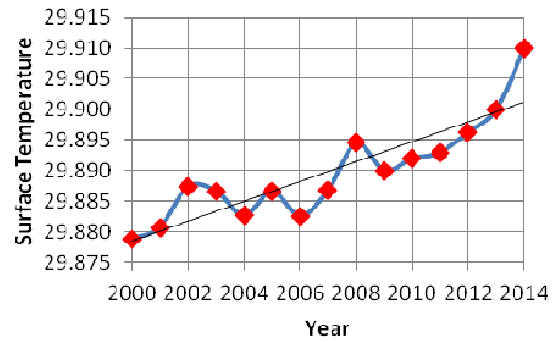


Fig. 12 Surface Temperature Trend

2006 shows increase in temperature in the 5 Local Government Areas of the study. With temperature curve at different landuse types shown in Fig. 11, the high density settlement areas still remained the area with the highest surface temperature and waterbody the least.

The trend of temperature curve in 2013 remained the same with high temperature corresponding to low and high settlement areas in Ibadan. Lowest temperature located towards the western part of Ibadan corresponds to areas that are densely vegetated and also consists of waterbody.

Fig. 12 shows the surface temperature trend between 2000 and 2014. It can be observed that there is an increase in temperature, ranging from the initial value of about 29.879°C to 29.91°C which is mainly due to urbanization.

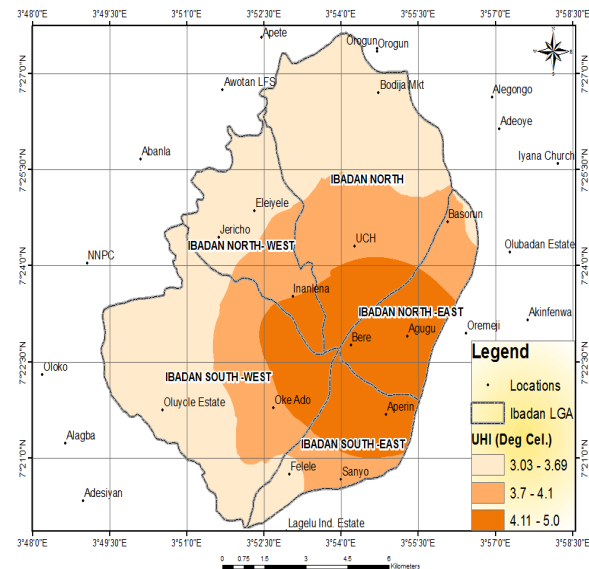


Fig. 13 Urban Heat Intensity (UHI)

### C. Assessment of UHI

The result of the UHI as shown in Fig. 13 indicates high values ranging from 4.11-5.0°C which is located at the central area and tend towards the south-east while the areas with low values ranges from 3.03-3.69°C. Fig. 14 showed that the urban heat intensity appears to be at its peak at the high density settlement areas with an average value of 4.9°C, while that of the low density settlement areas have an intensity of 4.7°C. Waterbody seems to have the least intensity of about 3°C and that of vegetation about 3.2°C. Overall, the urbanized areas which represent the LULC settlement classification displayed high UHI due to the presence of paved surfaces, corrugated roofing sheets and other man-made features.

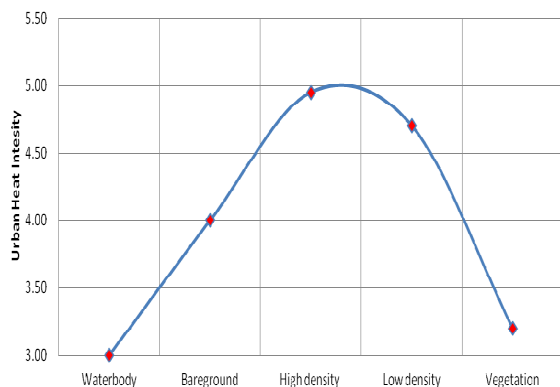


Fig. 14 Urban Heat Intensity (UHI) Values

### D. Examining Relationship between Landuse and Surface Temperature

The result showed that there is increase in surface temperature of waterbody from 1984 to 2000 as shown in Fig. 15. In 1984, the mean surface temperature was 19.03°C which increased to about 20.35°C indicating an increment of about 1.32°C increment in the surface temperature. This further increased to 20.37°C by the year 2006 and remained the same in 2013.

The bareground/rock outcrop also showed increase in surface temperature by 0.43°C during the years of study. It was observed that the surface temperature was 23.80°C in 1984 and further increased to about 24.20°C by 2000 and by 2013; it had increased by 0.9°C.

High and low density settlement areas showed similar trend in surface temperature, as the surface temperature values of the high density areas showed that in 1984, the value was 27.20°C which further increased to 28.10°C in 2000 and by 2013, surface temperature had increased to 28.80°C. The low density areas showed that the initial surface temperature in 1984 was 26.4°C and it increased to 27°C in 2006 and by 2013, the surface temperature was 27.40°C.

Vegetated area in 1984 had a surface temperature value of 22.20°C which increased to 22.21°C in 2000 while in 2013; the surface temperature is about 22.24°C.

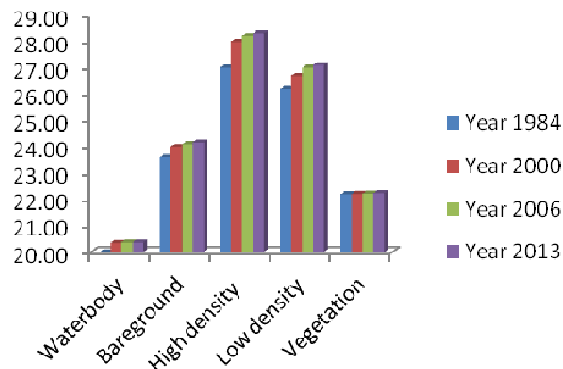


Fig. 15 Surface Temperature Values

### V. CONCLUSION

The above discussion has evaluated the effect of different landuse types on Land Surface Temperature. The main findings of the study have fulfilled the aim and objective of this research. Through this analysis, the change pattern of different landuse/landcover type was studied. This study introduces a methodology using combination of RS/GIS techniques to update landuse change database.

The change rates of the major landuse types from 1984 to 2013 which have decreased are vegetation and waterbody. However, the low and high density settlement and bareground/rock outcrop areas increased. The spatio-temporal variation of temperature result showed that temperature has increased overtime and the Urban Heat Intensity (UHI) appears to be at the peak in the high density settlement areas with intensity value of about 4.9°C while the least value of intensity at the vegetated and waterbody areas were observed to be around 3.0°C.

Conclusively, there is an obvious growth in settlement areas of Ibadan and the growth played a major role in the increase of temperature values.

### VI. RECOMMENDATION

It is recommended to study LST with a high resolution satellite image and carry out the similar studies for other Local Government Areas. Studying seasonal changes in LST and relating it to landuse patterns is recommended. This study will be a significant endeavor in promoting global and regional climatic models. It would be beneficial to the urban planners for future land use planning. Moreover, this research will provide guidance on how to manage thermal environment of big cities in accordance to landuse management.

### ACKNOWLEDGMENT

The author thanks to the various institutions for their support during the course of this research.

### REFERENCES

- [1] A.J. Amfield, "Two decades of urban climate research: a review of turbulence, exchanges of energy and water, and the urban heat island". International Journal of Climatology, 2003, 23, pp. 1-26.

- [2] D.A. Artis and W.H. Camahan, "Survey of emissivity variability in thermography of urban areas". *Remote Sensing of the Environment*, 1982, 12, pp. 313-329.
- [3] H.E. Landsberg, "The urban climate". Academic Press: New York, NY, USA, 1981, pp. 84-89.
- [4] Landsat Project Science Office. Landsat 7 science data user's handbook (Goddard Space Flight Center) 2001. Available online at: [http://Landsathandbook.gsfc.nasa.gov/handbook\\_html/chapter/chapter11.html](http://Landsathandbook.gsfc.nasa.gov/handbook_html/chapter/chapter11.html) (accessed 15 September, 2010).
- [5] Y. Ma, Y. Kuang and H. Ningsheng, "Coupling urbanization analysis for studying urban thermal environment and its interplay with biophysical parameters based on TM/ETM+ imagery". *International Journal of Applied Earth Observation and Geoinformation*, 2010, 12, pp. 110-118.
- [6] J.J. McCarthy, V.D. Canziani, F.Osualdo, N.A. Leary, D.J. Dokken and K.S. White (ed), "Climate change 2001: Impacts, adaptation and vulnerability: summary for policy makers", 2001.
- [7] NASA. The Enhanced Thematic Mapper Plus. Available online at: <http://Landsat.gsfc.nasa.gov/about/etm+.html> (accessed 15 December 2010).
- [8] J.E. Nichol, "A GIS-Based approach to microclimate monitoring in Singapore's high-rise housing estates". *Photogrammetric Engineering and Remote Sensing*, 1994, 60, pp. 1225-1232.
- [9] T.R. Oke, "The energetic basis of the urban heat island". *Quarterly Journal of the Royal Meteorological Society*; 1982, 108 (455) 1-24.
- [10] M. Stathopoulou, C. Cartalis and M. Petrakis, "Integrating corine landcover data and Landsat TM for surface emissivity definition: Application to the urban area of Athens, Greece". *International Journal of Remote Sensing*, 2007, 28, 3291-3304.
- [11] J.A.Voogt and T.R. Oke, "Thermal remote sensing of urban climates". *Remote Sensing of Environment*, 2003, 86, pp. 370-384.
- [12] URL:<http://www.glcapp.umiacs.umd.edu:8080/esdi/index.jsp>.